ELSEVIER

Journal of Non-Crystalline Solids 231 (1998) 209–221

JOURNAL OF NON-CRYSTALLINE SOLIDS

Ab initio cluster simulation of N-doped tetrahedral amorphous carbon

Ariel A. Valladares [a,*], Alexander Valladares [a], Renela M. Valladares [b], Mary A. McNelis [c]

[a] *Instituto de Investigaciones en Materiales, UNAM, Apartado Postal 70-360, 04510 México D.F., Mexico*
[b] *Facultad de Ciencias, UNAM, 04510 México D.F., Mexico*
[c] *Apartado Postal 70-464, 04510 México D.F., Mexico*

Received 9 September 1997; received in revised form 5 February 1998

Abstract

The electronic structure of nitrogen-doped tetrahedral carbon clusters, both amorphous and crystalline, with 21, 57 and 59 carbon atoms and various ring topologies, were studied using the self-consistent ab initio density functional theory-local density approximation (DFT-LDA). All clusters were hydrogen saturated. Clusters with $n = 0, 1$ and 4 nitrogen atoms were analyzed for each structure using an initial interatomic distance of 0.154 nm as in the bulk. All clusters were energy optimized maintaining tetrahedral symmetry and the position of the outermost atoms in order to simulate the inertia of the bulk. For all the clusters the energy gap increases with one N. For the 21-atom cluster which contains only 6-atom boat-rings the gap remains practically constant as n increases from 1, 6.60 to 4, 6.51 eV, unlike the other clusters. The Fermi energy varies from the top of the valence band to the bottom of the conduction band as the nitrogen concentration increases. In the forced fourfold coordinated environment N is a shallow donor as is P in Si; however, when N becomes essentially threefold coordinated, states appear in the middle of the gap.

PACS: 71.55.J; 71.10; 61.71

1. Introduction

Carbon and its many combinations and phases have always enriched the world of chemistry. Being one of the simplest elements, the variety of compounds that it generates and the several phases in which it manifests itself is simply astonishing. It is known that this versatility is to a large extent due to the different types of bonding that the element can display which allow for linear, planar and 3-dimensional structures. Recently a new form has been identified and this material is now known as tetrahedral amorphous carbon (ta-C). In 1991 thin films of ta-C were grown by McKenzie et al. [1], thereby confirming the existence of this amorphous form of diamond originally produced as hard carbon coatings in 1978 [2]. This form of amorphous carbon has more than 85% fourfold coordinated atoms.

Amorphous carbon is a material in which both sp^3 and sp^2 hybridizations coexist [1]. Attempts to determine its structure have produced results that

* Corresponding author. Present address: Molecular Simulations Inc., 9685 Scranton Road, San Diego, CA 92121, USA. Tel.: +52-5 622 4636; e-mail: valladar@servidor.unam.mx.

0022-3093/98/$19.00
PII: S0022-3093(98)00448-7

indicate a wide spectrum of bonding types, coordination numbers and bonding angles, that make experimental and theoretical studies sample dependent [3]. In ta-C films there are essentially sp^3 bonds that give them the diamond-like properties of hardness, density, and chemical inertness. The bond length, bond angle and coordination number of these films are 0.153 nm, 110° and 3.7, respectively, determined from neutron scattering experiments [4], in comparison to 0.154 nm, 109.47° and 4.0 for diamond and 0.142 nm, 120° and 3.0 for graphite. This leads to an sp^3 hybridization in ta-C of 86% and, in some cases reported recently, more than 90% (see [5] and references contained therein for a current account). ta-C is a semiconductor with a band gap [1] of ~ 2.0 eV [6], in comparison to 5.5 eV for the indirect energy gap in diamond [7] and practically 0.0 eV for graphite. It contains very little hydrogen so it should not suffer from any of the hydrogen-related instabilities exhibited by a-Si:H [8]. McKenzie et al. also found a uniform distribution of the dihedral angles, characteristic of all amorphous tetrahedrally bonded semiconductors. These properties makes it amenable for a cluster simulation of pure and doped amorphous samples.

Being a novel material ta-C has only recently been doped with phosphorus and nitrogen [9]. The results for the nitrogen-doped samples show that from the estimated value of 2.0 eV for the pure material, the gap increases to 2.2 eV for very low concentrations (10^{-3}) and remains constant up to 1%. At higher concentrations the sp^2 component of both C and N increases producing a C–N alloy and the percentage of fourfold bonds diminishes; the optical gap also decreases and for 10% nitrogen the value reported is $\sim$1.5 eV [9]. It has been argued [9] that the initial increase in the size of the gap is due to nitrogen passivation of the dangling bonds that exist in ta-C, thereby cleaning the gap and increasing it, and that the constancy of the gap at concentrations $\leqslant 10\%$ is due to the incorporation of N substitutionally in the ta-C network, since both elements have similar electronic structures. The position of the Fermi level of the samples varies from near the top of the valence band edge for the pure, to midgap and then to close to the conduction band mobility edge for the highly doped. It is said that the Fermi level in the pure material is pinned by defects (neutral dangling bonds) to states barely above the valence band and as the impurity concentration increases the defects heal, bringing the Fermi level down to the top of the valence band and then the level systematically increases with the concentration. Nitrogen becomes a shallow donor, effectively doping the ta-C, unlike the crystalline case for which nitrogen is a deep donor, 1.7 eV below the bottom of the conduction band. This is a remarkable result since for decades it has been known that N is a deep impurity in crystalline C whereas P is a shallow impurity in Si, a fact that is now explained by proposing that nitrogen in crystalline carbon relaxes into a threefold coordinated impurity that generates states within the energy gap [10].

The decreasing trend of the gap as the amount of nitrogen approaches 10% is attributed [3] to substantial bandtailing caused by the sp^2 bonds that appear however small their concentration, since it is said that the π and π^* states generated in this type of bonding show up at the top of the valence band and the bottom of the conduction band, respectively, thereby decreasing the gap [11]. Also, the appearance of these conduction band tail states which seem to push this band to smaller energies makes N a shallow donor, assuming that the impurity level does not change with respect to the unaltered conduction band. Similar arguments have been used to understand the variations of the gap for pure amorphous carbon samples, both tetrahedrally bonded and otherwise, hydrogenated and non-hydrogenated [3]. For these materials the optical (Tauc) gap seems to vary with sp^2 content z as: $E_g = 3.0 - 2.5z$ eV and, in particular, the optical gap of ta-C also varies in this manner as a function of z. In fact, in Ref. [3] the coefficient of z is -0.5 which does not seem to fit the data reported there in Fig. 4. It is clear from this equation that for a completely fourfold coordinated amorphous carbon sample (100% sp^3 bonding) one would expect a pure gap value of 3.0 eV and for a completely threefold coordinated

[1] In Ref. [5] an E_{04} gap as large as 2.85 eV for highly tetrahedral *hydrogenated* amorphous carbon is reported.

amorphous carbon sample (100% sp^2 bonding, essentially graphite), a value of 0.5 eV.

Recently there have been density-functional molecular dynamics calculations of ta-C:N within the local density approximation and the non-local pseudopotential scheme [12], using four pseudo-atomic orbitals per site with a confinement range of $r_C = 4.1a_B$ and $r_C = 3.75a_B$ for carbon and nitrogen, respectively. This ab initio local basis density functional (LBDF) method was applied to a 64 atom cell with four nitrogen concentrations: 1/64, 2/64, 3/64 and 6/64, [12]. They found that their cell contained dangling bonds, strained or stretched bonds and some threefold coordinated carbons or nitrogens. For example, the cell with a concentration of 9.38% had a structure with about 22% threefold coordinated atoms, that is, 22% of sp^2 bonds, and most of these defects occurred in π-bonded pairs or formed triplets with already existing π-pairs. The C π-pair had a planar graphitic structure but no additional information was given concerning the topology of the rings in their cell.

It is well known that density functional methods tend to understimate the size of the gap [13]; however, Stumm and Drabold [12] point out that their LBDF method, due to the use of a minimal local basis set, tends to slightly overestimate the gap value. Their results indicate that there is no localization on eigenstates around the gap associated with the nitrogen site unless it is threefold coordinated, that nitrogen induces disorder in the network but locally adapts to the bonding environment of the carbon atom which it substitutes and that, for all calculations, introducing nitrogen leads to a reduction of the band gap. They also found that the different kinds of defects are localized on states in the valence and/or conduction band, but threefold coordinated defects tend to be more often localized as midgap states or in the conduction band; the clustering of nitrogen atoms in π-bonded atom sites is energetically favored over substitution into a diamond-like environment and does not result in additional gap states. Recent work by Stumm et al. [14] using the same method and the same parameters, but now applied to a structural model with 216 atoms, indicate that the nitrogen occuring in tetrahedral sites or chains of an even number of π-bonded sites results in an increase in the Fermi energy, while its incorporation in strained network sites induces structural changes that lead to an increase in the sp^2 fraction of the material. Electrical conduction mechanisms are also discussed. Weich et al. [15] report calculations of several samples of C–N where an analysis of the influence of ring topology on its properties, in particular its relationship to the hardness of the material, is carried out.

In this scenario we decided to study the effect of nitrogen addition in a constrained tetrahedrally symmetric cluster environment: a fourfold coordinated one in which nitrogen substitutes carbons initially without altering the coordination number of 4, thereby starting with a ta-C-like structure. In this paper we present the results of an extensive ab initio DFT-LDA investigation of the effect of nitrogen on the electronic structure of carbon clusters with 21, 57 and 59 carbon atoms, both amorphous and crystalline, with 6-atom boat-type rings, with both 6-atom boat-type and 5-atom rings, and 6-atom chair-type rings, respectively, all hydrogen saturated. Clusters with $n = 0, 1$ and 4 nitrogen atoms were analyzed for all structures and the initial interatomic distance used was 0.154 nm as in the bulk. All clusters were geometry optimized maintaining tetrahedral symmetry and, to simulate the inertia of the bulk and to avoid spurious changes introduced by possible motion of the hydrogens, the positions of the outermost layers of C were kept fixed, and also those of the H atoms whenever possible. The study of clusters can shed new light on these problems since it allows the analysis of particular properties, specific restrictions or geometries that may contribute to discern the role of different factors that are relevant to the electronic structure of these materials. Section 2 contains a description of the three types of clusters used in this work, emphasizing the nature of the ring topology, the amorphous or crystalline characteristics and their geometry. Section 3 contains a description of the ab initio DFT-LDA self-consistent *DMol* method used in our calculations. In Section 4 we present our results and discussion comparing them to experiment and theory. Section 5 contains the conclusions of our work.

2. The clusters

All the clusters were constructed using the Builder Module within the *InsightII* graphical user interface of MSI [16]. We constructed three basic classes that are identified by the number of carbon atoms in the pure ones: the C21 cluster which has 28 hydrogen saturators, the C57 cluster with 52 hydrogen saturators and the C59 cluster with 60 hydrogen saturators. The total number of atoms in the clusters is therefore: 49, 109 and 119, respectively. When nitrogen was incorporated substitutionally the clusters were then identified by mentioning explicitly the number of each species; for example, C53N4 is the cluster that contains 53 carbons and 4 nitrogens and thus belongs to the C57 class with a total of 109 atoms. The energy optimization was carried out using the *DMol* program within the ab initio DFT-LDA self-consistent approximation for both restricted and unrestricted spins.

2.1. The C21 clusters

Although the C21 clusters used in this work were constructed with the Builder Module of *InsightII* [16], they are similar to the ones utilized in our previous work [17]; the Builder allows better precision in the construction. These amorphous clusters have 6-atom boat-type rings that are found in amorphous solids but never in crystalline ones, the coordination number is 4 and they have tetrahedral symmetry. The cluster (Fig. 1) has a central atom, 4 nearest neighbors, *nn*, 12 second neighbors, 2*n*, and 4 third neighbors, 3*n*. All interior angles of the 6-atom rings are 109.47° and the interatomic distances are 0.154 nm before energy optimization. The cluster was hydrogenated and the H atoms were placed at a distance of 0.107 nm, without altering the tetrahedral symmetry; it has the symmetry of the T_d point group with eight degrees of freedom.

For the smallest concentration, one nitrogen was placed at the center of the cluster, substituting a carbon; for the next concentration 4 nitrogens were placed in the *nn* positions substituting carbons. The geometry optimization was carried out for C21, C20N1 and C17N4 maintaining the 2*n* atoms, the 3*n* atoms and the hydrogens fixed.

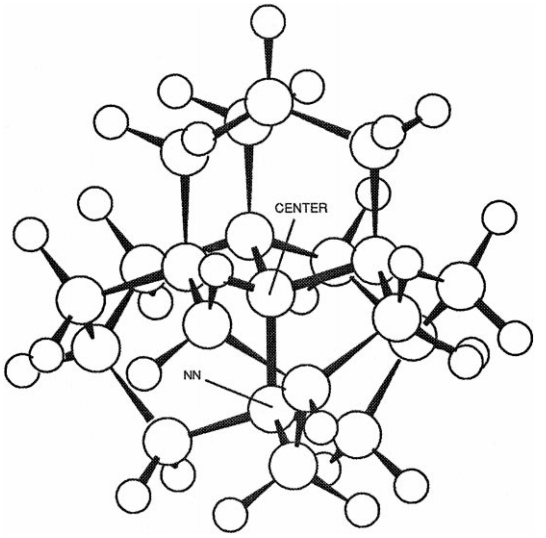

Fig. 1. C21 cluster which contains only 6-atom boat-type rings with a central atom, 4 *nn*, 12 2*n* and 4 3*n*. The cluster has the symmetry of the T_d point group with eight degrees of freedom. The 28 hydrogen atom saturators are indicated as small circles.

2.2. The C57 clusters

To see the effect of the simultaneous presence of 5-atom planar rings and 6-atom boat-type rings on the electronic properties we constructed a larger cluster that combines both features. Starting with the C21 cluster, a layer of 6 pentagons tetrahedrally arranged was added around each *nn* atom, adequately adjusting the five interior angles of a given 5-atom ring: one of 109.47° at the common vertex of the six pentagons, two of 106.84° closest to the previous angle and the remaining two of 108.425°. The interatomic distances are all 0.154 nm before energy optimization. An additional outermost layer of 6-atom boat-type rings was constructed and hydrogens were also placed at a distance of 0.107 nm from the carbons, always maintaining a coordination number of 4 and tetrahedral symmetry. The cluster (Fig. 2) has a central atom, 4 *nn*, 12 2*n*, 4 3*n*, 24 4*n* and 12 5*n*; it has the symmetry of the T_d point group with 17 degrees of freedom.

Again, two concentrations were studied, that with one nitrogen at the center of the cluster substituting a carbon, and that with 4 nitrogens in the *nn* positions, substituting carbons. The geometry

optimization was carried out for C57, C56N1 and C53N4 maintaining the 2*n*, 3*n*, 4*n* and 5*n* atoms fixed. Due to the fact that the maximum number of constraints in *DMol* did not allow us to fix all the hydrogens, we optimized the pure carbon cluster with the hydrogens and the *nn* free. The geometry thus found was used as the basic cluster for the impure runs. After every impure optimization the positions of the hydrogens with respect to the carbons were measured and were found to remain constant within one part in 110.

2.3. The C59 clusters

Finally, to see the effect of crystallinity and compare it with the amorphous state of the previous clusters we constructed a crystalline one with only 6-atom chair-type rings, the only type of ring present in the crystal, with the interatomic distances of the bulk and fourfold coordinated. We then substituted one nitrogen at the center and 4 nitrogens at the *nn* position, as above. The cluster (Fig. 3) has a central atom, 4 *nn*, 12 2*n*, 12 3*n*, 6 4*n*, 12 5*n* and 12 6*n*; it has the symmetry of the T_d point group with 20 degrees of freedom. The hydrogens were placed at a distance of 0.107 nm from the carbons, always maintaining a coordination number of 4 and the tetrahedral symmetry.

The geometry optimization was carried out for C59, C58N1 and C55N4 maintaining the 2*n*, 3*n*, 4*n*, 5*n* and 6*n* atoms fixed. Once again, as for the C57 cluster, the pure carbon cluster was optimized with the hydrogens and the *nn* free and the geometry found was used as the basic cluster for the impure runs. After every impure optimization we measured the position of the hydrogens and found that the distances remained constant within one part in 110.

3. The method

In the present work we have used the density functional theory (DFT) approach of Hohenberg and Kohn, and Kohn and Sham [18] implemented in the *DMol* code [13] which treats the electronic

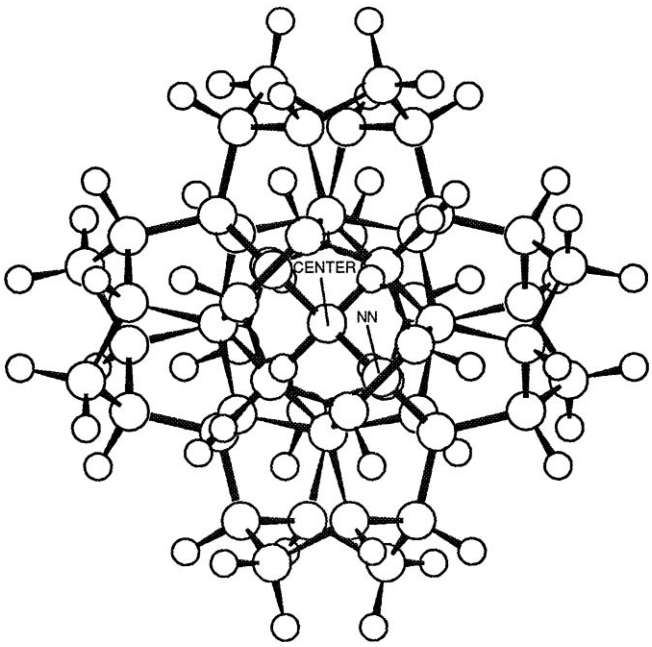

Fig. 2. The C57 cluster combines 6-atom boat-type rings and 5-atom planar rings. It contains a central atom, 4 *nn*, 12 2*n*, 4 3*n*, 24 4*n* and 12 5*n* and has the symmetry of the T_d point group with 17 degrees of freedom. There are 52 outermost hydrogen saturators depicted.

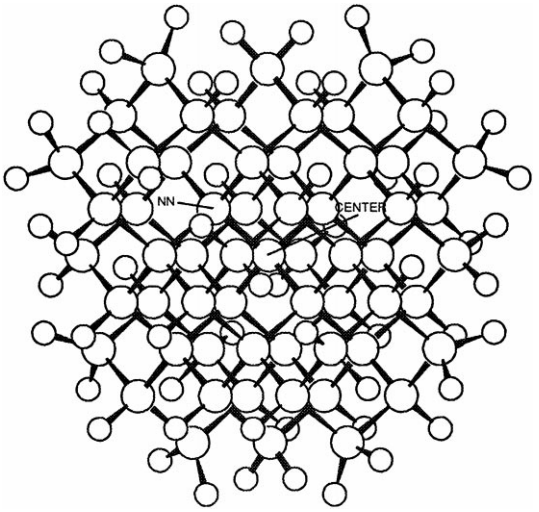

Fig. 3. This crystalline cluster C59 has a central atom, 4 *nn*, 12 2*n*, 12 3*n*, 6 4*n*, 12 5*n* and 12 6*n*; it has the symmetry of the T_d point group with 20 degrees of freedom and 60 outermost hydrogen saturators.

structure of molecules or clusters by solving the Kohn–Sham self-consistency equations within local or non-local density approximations. In our work we used the local density approximation (LDA) of Vosko et al. (VWN) [19]. *DMol* calculates the solutions to the DFT equations variationally and self-consistently and these solutions provide the molecular wave functions and electron densities which can be used to evaluate the energetics and the electronic and magnetic properties of the system. In this paper we report the results of the density of states calculations that are necessary to study the behavior of the forbidden energy gap, the position of the Fermi level and the impurity levels, and their implication for the shallowness or for the depth of the nitrogen energy levels in the various clusters.

DMol employs a real space method with numerical basis functions centered on the atoms and this procedure allows systems larger than those that would be possible with other ab initio techniques for comparable computational costs. This code also allows the calculation of the electronic properties both for spin restricted and spin unrestricted systems, and since we have closed and open shell clusters, both types of calculations were carried out. The electron gas exchange-correlation energy in *DMol* is based on the work of von Barth and Hedin [20]; the exchange energy is spin independent and the correlation contributions depend upon whether the computation is spin restricted or spin unrestricted [13].

The solutions to the Kohn–Sham equations generate interatomic forces and the evaluation of the energy gradients provides a convenient method for determining the equilibrium geometry of the system, free or subject to constraints. In fact, *DMol* includes a suite of algorithms for geometry optimization that locates both minima and transition states on a potential energy surface. The core of the program is the so-called Eigenvector Following algorithm (EF) proposed by Baker in 1986 [21]. It can optimize in cartesian coordinates or in a set of non-redundant internal coordinates that are generated automatically from the cartesian coordinates used as input. It can also handle fixed constraints on distances, bond angles and dihedral angles. The process is iterative, with repeated calculations of energies and gradients and calculations, or estimations, of hessians in every optimization cycle until convergence is attained.

Recent calculations in silicon [22] have shown that the energy gap value changes only marginally when using different approximations at the local level and since we are concerned here with tendencies, and not with the absolute values of the gaps, we used the VWN approximation throughout. We also used a double numerical basis set that includes d-polarization of the atoms (DND) and the frozen inner core orbitals approximation; a medium grid was used for the numerical calculations since we were looking for consistent trends of the properties of these clusters as a function of concentration. The SCF density parameter that specifies the minimum degree of convergence for the LDA density was set at 10^{-6}.

4. Results and discussion

The difficulty in dealing theoretically with covalently bonded disordered materials is well known and has limited progress in the area. The use of a chemical approach to the subject [3,11]

gives insight into the local (atomic) nature of the problem whereas the supercell approach [12,14] combined with annealing and quenching cycles gives information of possible structures in which these amorphous materials may be found. The relevance of both lines of attack is clear and both have given important information concerning the processes that take place in ta-C:N. However, the study of clusters is a different approach that can shed new light on these problems since it allows the analysis of particular characteristics, specific restrictions or geometries that may contribute to understanding and discerning the role of different factors, relevant to the electronic structure of these materials, on a larger than atomic scale and without periodic boundary conditions.

In this work the three basic types of tetrahedral clusters constructed emphasize properties that are expected to occur in amorphous carbon nitride and to study the effect of these properties on the electronic properties of ta-C:N. The effect of amorphous 6-atom boat-type rings has been studied by us, within the SCF pseudopotential Hartree–Fock approach, for a variety of impurities (N, P, As, B and Al) in both silicon and germanium [17] and the results are relevant for the doping properties of some of the impurities in spite of the qualitative nature of the Hartree–Fock method. In constructing the C57 clusters we discovered that the coexistence of 6-atom boat-type and 5-atom planar rings is very natural and this implies that whenever there are boat-type rings with 6 atoms it is probable to find planar rings with 5 atoms; clusters with alternating layers of these two types of rings can be readily formed. We wanted to analyze the effect of 5-atom rings because in doped amorphous carbon, pyrrole-like structures may appear with one nitrogen and four carbons in a pentagonal ring. Furthermore the presence of this type of ring may introduce dihedral angles that are different from the eclipsed and staggered ones generated by 6-atom chair-rings and 6-atom boat-type rings, respectively. It is well known that the 6-atom chair-type rings, which are the building blocks of crystalline solids, can also be found in amorphous materials and that is why it was important to carry out studies on the C59 which has only crystalline properties.

The pure carbon clusters were geometry optimized subject to the constraints mentioned in Section 2 and it was found that the center to nearest neighbor distances, *c–nn*, and the nearest neighbor to second neighbor distances, *nn–2n*, did not change more that 2 parts in 154, maintaining the basic structure of the original clusters. Once the clusters were contaminated with one and four nitrogens, the geometry optimization gave two types of results: for the C57 and C59 clusters the *c–nn* and *nn–2n* bond lengths did not vary more than 3 parts in 154, but for the C20N1 and C17N4 clusters there were some important differences, namely, *c–nn* changed to 0.158 and 0.183 nm and *nn–2n* changed to 0.152 and 0.147 nm, respectively. These changes are a relevant variation of the bond length for the electronic properties of the impure C21 clusters. Also, the angles *c–nn–2n* and *2n–nn–2n* varied from 109.03° and 109.91° for the geometry-optimized pure, to 107.95° and 110.94° for C20N1, and to 98.82° and 117.69° for C17N4, respectively. For this last cluster it is clear that the 4 nitrogens located in the *nn* positions have relaxed away from the central carbon to such a point that they are only 8.82° from being in the plane defined by the three *2n* carbons, and 2.31° of being essentially threefold coordinated; the bond length changed by almost 20%. This change indicates that the existence of 6-atom boat-type rings gives flexibility to the random network since they allow large relaxations of the atomic positions. When these rings are combined with pentagons, the network becomes more rigid and there are no such large relaxations; this rigidity is also present in the crystalline cluster. In all clusters the position of the *nn* is such that it could permit their displacement, were it not for the type of rings that bind them. For all clusters, pure and impure, we have studied the density of states curves, the variation of the gap size, the position of the Fermi level and the depth of the impurity levels for the relaxed geometry.

4.1. Density of states

To obtain global information of the electronic properties of the clusters it is necessary to construct the total density of states, DOS, for each one of them. Even though partial densities of

states and optical properties were also calculated, we are reporting here only the results for the total density of states and the energy level information that it contains.

To understand the DOS curves and the calculation of energy gaps, activation energies and depths of the donor states we have to identify adequately the highest occupied molecular orbital and the lowest unoccupied molecular orbital, or HOMO and LUMO, respectively, in the chemistry parlance, and also the impurity levels. The definition of an energy gap is very clear in the pure clusters; it is simply the energy difference between the HOMO and the LUMO. However, when looking at the experimental results it becomes apparent that for impure materials there are other parameters that enter into consideration. Thus, it is common to refer to the impurity levels as states localized within the energy gap and then one has to be careful with the HOMO and LUMO interpretation since in these circumstances the HOMO would become the highest occupied impurity level and the LUMO would be the lowest unoccupied impurity level which, in general, are very close to one another and certainly do not represent the quantities measured experimentally. Since the unrestricted spin option of *DMol* was used, α and β orbitals were obtained for the same spatial molecular orbital and we averaged the energy values of the symmetrically identical orbitals to give a single value for the gap, for the impurity levels and for the depth of the donor states.

In Figs. 4–6, the total densities of states for C21, C57 and C59, respectively, are shown. In Tables 1–3, all the values obtained directly from the runs and the average values for the pertinent energy levels are given. It can be seen that the top of the valence band, the HOMO, of each type of cluster moves systematically to smaller energies as the nitrogen concentration increases; on the other hand, the LUMO does not present this systematic variation. The density of states curves do not show clearly these tendencies since the half-width of the gaussians used for energy levels was chosen as 0.4 eV to better represent a continuous curve as in the bulk. Almost all the impurity levels, completely filled or half-filled, are located close to and below the bottom of the conduction band, the exception

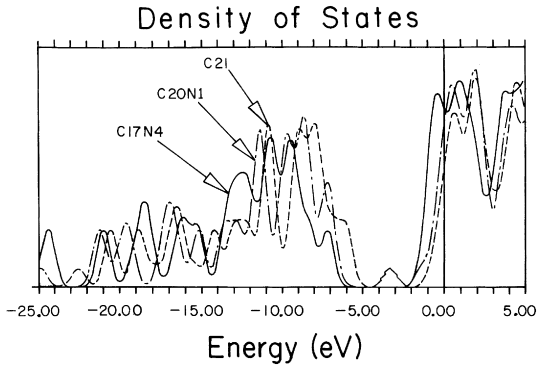

Fig. 4. DOS for C21, C20N1 and C17N4. The top of the valence band moves down to lower energies as the concentration increases. An impurity state can be clearly seen within the gap for C17N4.

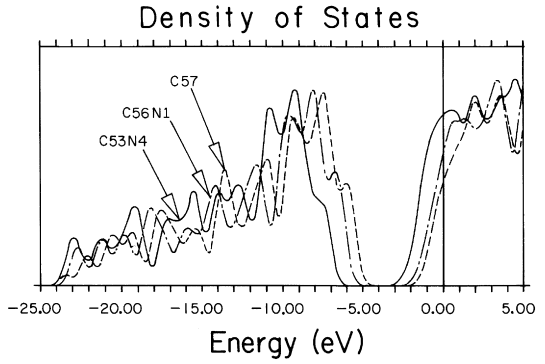

Fig. 5. DOS for C57, C56N1 and C53N4. The top of the valence band moves down to lower energies as the concentration increases.

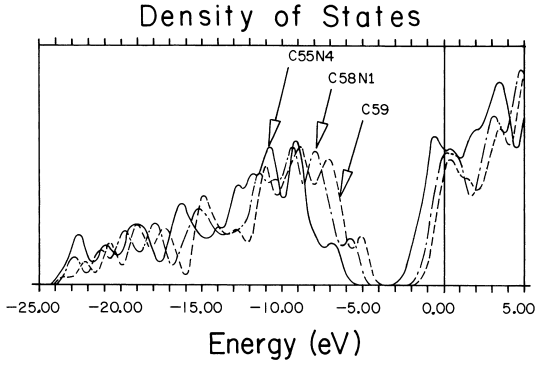

Fig. 6. DOS for C59, C58N1 and C55N4. The top of the valence band moves down to lower energies as the concentration increases.

Table 1
HOMO, LUMO and impurity levels: 49-atom clusters

Cluster type	Energy levels (eV), symmetry, occupancy		
	HOMO	LUMO	Impurity levels
C21	−6.055, T2, 6	−0.633, A1, 0	
C20N1	−7.043, T2, 3 −7.010, T2, 3 Average = −7.03	−0.494, T2, 0 −0.362, T2, 0 Average = −0.43	−1.421, A1, 1 −1.294, A1, 0 Average = −1.36
C17N4	−7.288, T2, 3 −7.140, T2, 3 Average = −7.21	−0.818, T2, 0 −0.589, T2, 0 Average = −0.70	−3.451, A1, 1 −3.207, A1, 1 Average = −3.33 −1.191, A1, 1 −1.004, A1, 0 Average = −1.10 −1.073, T2, 1 −0.850, T2, 0 Average = −0.96

Table 2
HOMO, LUMO and impurity levels: 109-atom clusters

Cluster type	Energy levels (eV), symmetry, occupancy		
	HOMO	LUMO	Impurity levels
C57	−5.710, T2, 6	−1.031, A1, 0	
C56N1	−6.327, T1, 3 −6.317, T1, 3 Average = −6.32	−0.965, T2, 0 −0.886, T2, 0 Average = −0.93	−1.456, A1, 1 −1.382, A1, 0 Average = −1.42
C53N4	−7.315, A2, 1 −7.297, A2, 1 Average = −7.31	−1.530, A1, 0 −1.427, A1, 0 Average = −1.48	−2.278, A1, 1 −2.186, A1, 1 Average = −2.23 −1.671, T2, 2 −1.547, T2, 0 Average = −1.61

Table 3
HOMO, LUMO and impurity levels: 119-atom clusters

Cluster type	Energy levels (eV), symmetry, occupancy		
	HOMO	LUMO	Impurity levels
C59	−5.036, T1, 6	−0.857, A1, 0	
C58N1	−5.522, T1, 3 −5.519, T1, 3 Average = −5.52	−0.984, T2, 0 −0.869, T2, 0 Average = −0.93	−1.309, A1, 1 −1.191, A1, 0 Average = −1.25
C55N4	−6.548, T1, 3 −6.543, T1, 3 Average = −6.55	−1.611, T2, 0 −1.579, T2, 0 Average = −1.60	−2.299, A1, 1 −2.136, A1, 1 Average = −2.22 −1.766, T2, 2 −1.690, T2, 0 Average = −1.73

being the impurity level corresponding to the A1 symmetric molecular orbital [23] with an energy of −3.33 eV in the C17N4 cluster, a level that is completely filled. The fact that the half-filled impurity levels are close to the bottom of the conduction band agrees with experimental results since it has been found that N is a dopant in ta-C:N for the lower concentrations.

The C17N4 impurity level that is found in the middle of the gap, −3.33 eV, is due to the almost threefold coordination of the nitrogens in this cluster. As mentioned above, the relaxed positions of these impurities is such that they are bonded to the central carbon atom and more strongly bonded to the three nearest carbons in the $2n$ positions; that is, there is one electron per atom in a semidangling state (the one directed towards the center of the cluster), and one electron in a dangling state. To investigate this point we optimized the C16N4 cluster which is the same as the C17N4 but with the central carbon atom removed; we found a geometry close to the one already described, which indicates that the presence or absence of the central carbon atom does not affect the geometry, but *does* affect the electronic structure of the cluster as can be seen in the resulting DOS curve represented in Fig. 7. This curve is different from the one in Fig. 4 and it shows states within the gap, due to the electrons now in dangling states. The unrestricted spin results give α and β orbitals that have the same energy for a given symmetry, just like the unrestricted spin results for closed shell systems. The numerical results indicate that in the −5.58 eV A1 orbitals 2 electrons can be allocated, and 6 electrons in the −3.84 eV T2 orbitals, both states within the gap. This allocation implies that threefold coordination of nitrogen generates states within the gap that are deep, as for the crystalline case [10]. *It is the existence of the weaker bond of the nitrogens with the central carbon (fourfold coordination) that gives rise to the shallow impurity levels.*

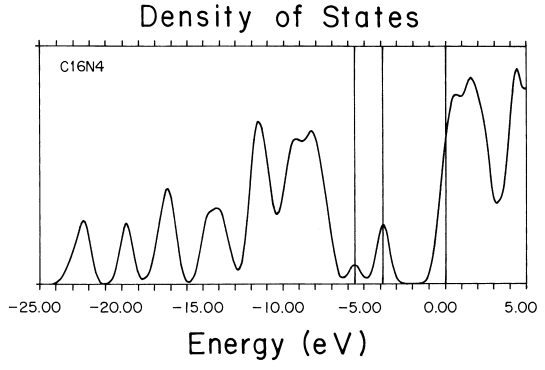

Fig. 7. DOS for the C16N4 cluster. This is the geometry-optimization of the C17N4 cluster without the center carbon atom. The states within the gap correspond to the 8 dangling electrons of the 4 nitrogens engaged in threefold bonding.

4.2. The energy gap

The energy gap of the pure clusters is defined as above; i.e., as the difference between the averaged HOMO and LUMO values. For the impure ones we define the energy gap in the following way: the energy of the highest molecular orbital below which the number of electrons is equal to the pure case corresponds to the new HOMO or the top of the valence band, E_v; having made this definition we account for the impurity levels which are symmetry-paired, as mentioned above, and usually very close to one another; the next molecular orbital is identified as the new LUMO or bottom of the conduction band with energy, E_c. The energy gap, E_g, is then equal to the difference $E_g = E_c - E_v$. Table 4 lists the gaps for the 9 clusters, and Fig. 8 shows the variation of the normalized gap as a function of nitrogen content. Since the term "concentrations" is inappropriate we have used the number of nitrogens as our content variable. In Fig. 9 we have graphed the variation of the gap with the number of carbon-plus-nitrogen atoms for the three amounts studied here. Several consequences can be drawn from this information.

Table 4
Energy gap values for the twelve clusters

Cluster type	Gap values (eV)		
	Pure	1 Nitrogen	4 Nitrogens
C21	5.42	6.60	6.51
C57	4.68	5.40	5.83
C59	4.18	4.59	4.95

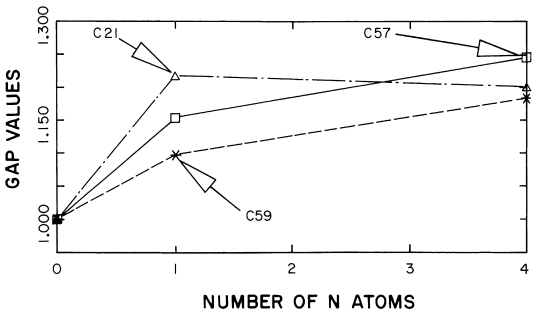

Fig. 8. Variation of the normalized gap as a function of nitrogen content. The gap for the C21-like clusters remains practically constant for one and four nitrogens, while the gap for the other clusters always increases.

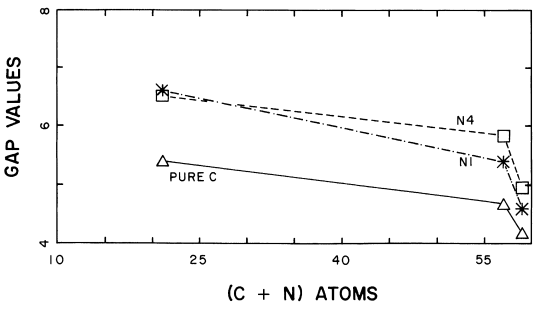

Fig. 9. Dependence of the gap on the number of carbon-plus-nitrogen atoms for the three concentrations studied here. It can be seen that the overall behavior of the *PURE* and 4N plots are very similar.

First of all, from Fig. 8 it is clear that for one nitrogen the gap is always larger than the value of the corresponding pure cluster; for four nitrogens the gap increases again for the C57 and C59 types of clusters in the following order: a 25% increase with respect to the pure for the C57, and then 18% for C59, whereas it remains essentially constant for the C21 cluster type, (22% for one nitrogen and 20% for four nitrogens), as has been reported experimentally. These numbers imply that according to our simulations the ta-C:N films must have a larger content of boat-like atom rings. The probability of finding a mixture of boat-type and 5-atom rings and 6-atom chair-type rings seems to be less and about the same for each one of these structures. Table 4 and Fig. 9 show unequivocally that the size of the gap decreases as the number of atoms in the clusters increases, both for pure and impure, which is to be expected since the larger the cluster the better it represents the bulk.

The calculated gaps for the pure C57 and C59 clusters are only about 220% larger that the experimental ones found for ta-C. Assuming that we can scale these gaps with respect to the experimental gaps we obtain that for C21 the factor is $2.00/5.42 = 0.37$; for C57 the factor becomes $2.00/4.68 = 0.43$ and for C59 $2.00/4.18 = 0.48$. This scaling factor gives us an idea of how close the theoretical results are to experiment.

4.3. The impurity levels

At $T = 0$ K the Fermi energy can be identified with the pinning energies of the highest occupied molecular levels. In Tables 1–3 we see how the position of the highest occupied molecular energy levels moves as a function of concentration. The highest occupied level for the pure clusters is the HOMO, which coincides with the top of the valence band. For the C21 clusters the displacement is from -6.06 eV for the pure, to -1.36 eV and to -0.96 eV as a function of the number of nitrogen atoms. For C57 the Fermi level varies from -5.71 eV, to -1.42 eV, and to -1.61 eV. Finally, for C59 the variation is from -5.04 eV to -1.25 eV, to -1.73 eV. This shows that indeed the Fermi level does vary from the top of the valence band to close to the conduction band as reported experimentally.

4.4. *Shallow* vs. *deep donors*

It is known that nitrogen in crystalline carbon is a deep donor and it has recently been stated that the difference between the behavior of P in Si and the corresponding case of N in C is that the isolated phosphorous in silicon is fourfold coordinated, whereas the isolated nitrogen in carbon becomes threefold coordinated [10]. It is argued that this state is due to the fact that the N wave function has a much greater localization which is deep-impurity-like even for the undistorted nitrogen [11].

However the recent experimental results for ta-C:N indicate the presence of shallow donor levels that makes nitrogen a dopant in this material.

The results that we obtained for clusters with fourfold coordination for all atoms, including nitrogen, also indicate the presence of shallow impurity levels introduced by this donor and its dangling bonds. In the clusters C57 and C59 the C–N distances do not vary more than 3 parts in 154; that is, less than 2% in the relaxed geometries. However in the C21 cluster the nitrogens relax to 0.183 nm from the center, stretching the bond 20%; this weak link generates states within the gap and also shallow impurity levels due to the fourfold coordination. Assuming that the gap scaling factors apply we find that the depth of the half-filled impurity levels goes from 0.05 to 0.34 eV and experimental results quote activation energies of the order of 0.6 eV for a 5% sample (see reference of S.R.P. Silva and G.A.J. Amaratunga in [9]). It is clear then that in a sample of ta-C:N the shallow levels of nitrogen are due to a well-defined fourfold coordination status of the nitrogen regardless of the topology of the rings, since threefold coordination would make it a deep donor, as shown in Fig. 9. This state is in contrast to the role that has been given to existing π and π^* bonds in these thin films as a mechanism for decreasing the bottom of the conduction band and for making the nitrogen level a shallow one. The constancy of the gap value for nitrogen doping has to be associated to the topology of the rings that are created in the growth process of the C–N samples, as seen in the C21 clusters.

5. Conclusions

Our results indicate that:

1. The DOS curves show a clean gap except for C17N4 for which there are strong threefold bonds in the cluster, although fourfold coordination is maintained with a stretched bond.

2. The energy gaps of all the clusters increase for $n = 1$, even though our clusters do not have any dangling bonds to passivate which is an argument used in the experimental papers to justify this increase [9]. For $n = 4$ the gap of the 21-atom boat-ring, C17N4, remains practically constant as in the experimental results [9], which indicates that this type of ring is likely to be found in the ta-C:N samples. The gaps of all the other clusters increase for $n = 4$ even though nitrogen enters substitutionally.

3. The Fermi energy varies from the top of the valence band to close to the bottom of the conduction band, going from the pure to the largest number, as reported experimentally [9]. The activation energies obtained, once they are scaled by the gap factor, are of the right order of magnitude as found experimentally.

4. Strong fourfold coordinated N (sp^3 bonding) is a shallow donor for all the clusters, with variations in the impurity levels that depend on the ring topology. Threefold coordinated nitrogen, as found in the C16N4 cluster, generates electronic states within the gap and is therefore a deep donor. It remains to contrast the relevance of this behavior with the behavior of the π and π^* bonds that appear in sp^2 bonding.

Acknowledgements

A.A.V. acknowledges the funding of DGAPA-UNAM to spend his sabbatical year at Molecular Simulations, Inc., and the support of MSI for this work; A.V. acknowledges DGAPA-UNAM for funding his graduate studies at the Department of Materials, University of Oxford, Oxford, UK. The computational results were obtained using the *DMol* code of Molecular Simulations Inc., San Diego, CA, USA. Some graphical displays were printed out from *InsightII* molecular modeling systems. Some were carried out by J. Camacho.

References

[1] D.R. McKenzie, D. Muller, B.A. Pailthorpe, Phys. Rev. Lett. 67 (1991) 773.
[2] I.I. Aksenov, V.A. Belous, V.G. Padalka, V.M. Khoroshikh, Sov. J. Plasma Phys. 4 (1978) 425.
[3] For a recent account of the pure amorphous carbon situation see J. Robertson, J. Non-Cryst. Solids 198 (1996) 615, and references contained therein.
[4] P.A. Gaskell, A. Saeed, P. Chieux, D.R. McKenzie, Phys. Rev. Lett. 67 (1991) 1286.
[5] M. Weiler, S. Sattel, T. Giessen, K. Jung, H. Ehrhardt, V.S. Veerasamy, J. Robertson, Phys. Rev. B 53 (1996) 1594.

[6] V. Veerasamy, G.A.J. Amaratunga, W.I. Milne, C. Davis, S.R.P. Silva, H. MacKenzie, Appl. Phys. Lett. 63 (1993) 370.
[7] O. Madelung (Ed.), Semiconductors-Basic Data, 2nd revised edition, Springer, Berlin, 1966, p. 6.
[8] W.I. Milne, J. Non-Cryst. Solids 198 (1996) 605.
[9] V.S. Veerasamy, G.A.J. Amaratunga, C.A. Davis, A.E. Timbs, W.I. Milne, D.R. McKenzie, J. Phys.: Condens. Matter 5 (1993) L169; V.S. Veerasamy, J. Yuan, G.A.J. Amaratunga, W.I. Milne, K.W.R. Gilkes, M. Weiler, L.M. Brown, Phys. Rev. B 48 (1993) 17954; C.A. Davis, D.R. McKenzie, Y. Yin, E. Kravtchinskaia, G.A.J. Amaratunga, V.S. Veerasamy, Philos. Mag. 69 (1994) 1133; D.R. McKenzie, Y. Yin, N.A. Marks, C.A. Davis, B.A. Pailthorpe, G.A.J. Amaratunga, V.S. Veerasamy, Diamond Rel. Mater. 3 (1994) 353; S.R.P. Silva, G.A.J. Amaratunga, Thin Solid Films 270 (1995) 194; S.R.P. Silva, B. Rafferty, G.A.J. Amaratunga, J. Schwan, D.F. Franceschini, L.M. Brown, Diamond Rel. Mater. 5 (1996) 401.
[10] S.A. Kajihara, A. Antonelli, J. Bernholc, R. Car, Phys. Rev. Lett. 66 (1991) 2010.
[11] J. Robertson, C.A. Davis, Diamond Rel. Mater. 4 (1995) 441.
[12] P. Stumm, D.A. Drabold, Solid State Commun. 93 (1995) 617.
[13] Quantum Chemistry, DMol User Guide, Release 960, Molecular Simulations, Inc., San Diego, September 1996; see also B. Delley, J. Chem. Phys. 92 (1990) 508 and J. Chem. Phys. 94 (1991) 7245.
[14] P. Stumm, D.A. Drabold, P.A. Fedders, J. Appl. Phys. 81 (1997) 1289.
[15] F. Weich, J. Widany, Th. Frauenheim, Phys. Rev. Lett. 78 (1997) 3326.
[16] Insight II User Guide, Release 4.0.0, Molecular Simulations, Inc., San Diego, September 1996.
[17] L.E. Sansores, A.A. Valladares, J. Non-Cryst. Solids 191 (1995) 227; J.A. Cogordan, L.E. Sansores, A.A. Valladares, J. Non-Cryst. Solids 181 (1995) 135; L.E. Sansores, R.M. Valladares, A.A. Valladares, J. Non-Cryst. Solids 144 (1992) 115; L.E. Sansores, R.M. Valladares, J.A. Cogordan, A.A. Valladares, J. Non-Cryst. Solids 143 (1992) 232.
[18] P. Hohenberg, W. Kohn, Phys. Rev. B 136 (1964) 864; W. Kohn, L.J. Sham, Phys. Rev. A 140 (1965) 1133.
[19] S.J. Vosko, L. Wilk, M. Nusair, Can. J. Phys. 58 (1980) 1200.
[20] U. von Barth, L. Hedin, J. Phys. C 5 (1972) 1629.
[21] J. Baker, J. Comput. Chem. 7 (1986) 385; see also J. Baker, D. Bergeron, J. Comput. Chem. 14 (1993) 1339.
[22] B. Delley, E.F. Steigmeier, Appl. Phys. Lett. 67 (1995) 2370.
[23] See F.A. Cotton, Chemical Applications of Group Theory, Wiley/Interscience, New York, 1971, for a detailed discussion of molecular symmetry as implemented in *DMol*.